

PHYSICAL REVIEW LETTERS

VOLUME 30

26 FEBRUARY 1973

NUMBER 9

Impact-Parameter Dependence of K -Shell Coulomb-Ionization Cross Sections*

Werner Brandt, † K. W. Jones, and H. W. Kraner
Brookhaven National Laboratory, Upton, New York 11973
(Received 22 November 1972)

Coincidence measurements are reported between the characteristic K -shell x rays emerging from a target and the protons of energy 0.3–3 MeV, scattered by 5° from an incident beam, that cause the primary K -shell ionization. Absolute impact-parameter-dependent differential K -shell ionization cross sections are deduced for Al, Ca, Ni, and Ag. In a reduced plot the data follow a common curve that coincides with the semiclassical prediction of Bang and Hansteen.

We report measurements by a coincidence technique of the differential K -shell ionization cross sections of target atoms of Al, Ca, Ni, and Ag, for 0.3–3-MeV protons as a function of the projectile impact parameter. Under these conditions Coulomb ionization dominates.¹ Our data, in conjunction with independent observations on Se, Cu, and Ag made by a somewhat different coincidence technique,² confirm the predictions of the impact-parameter-dependent cross sections derived by Bang and Hansteen.³ The measurements establish a firm basis from which the distinguishing characteristics of K -shell Pauli excitation^{1,4,5} can be gauged quantitatively and in detail.

For projectile velocities small compared to the relevant electron velocities in the target shells, one can consider two distinct ionization mechanisms. Projectiles (subscript 1) that act as bare, charged point particles produce holes in inner shells of target atoms (subscript 2) via Coulomb excitation. Projectiles that carry a coterie of electrons into the interaction region promote inner-shell electrons by virtue of the Pauli exclusion principle acting in the overlapping electron clouds of the collision partners. K -shell ionization cross sections under Pauli-excitation conditions are larger by orders of magnitude than the Coulomb-ionization cross sections

at the same projectile velocities.⁴ Decidedly, they cannot be accounted for by quantum-theoretical Coulomb-excitation cross sections.^{1,5} Nor can they be interpreted satisfactorily as being caused by electron promotion through diabatic crossings of the energy levels of the colliding atoms.^{6,7}

It is important, then, to progress from measurements of total ionization cross sections⁸ to experiments that can give detailed evidence for the distinction between Coulomb and Pauli excitation. One can make use of the fact that when electrons fill K -shell holes, with a certain fluorescence yield $\gamma_K < 1$, the atom emits a characteristic x ray. In classical terms, the projectile trajectory with impact parameter p bends in the field of the target nucleus through an angle ϑ that is related to p by Rutherford's scattering law. The ionization probability as a function of p can be determined via the yield of K -shell x rays measured in coincidence with the projectiles emerging from the target at the angle ϑ .⁴ At low particle velocities $v_1 \ll v_{2K}$, where $v_{2K} = Z_{2K}v_0$ is the velocity of the target-atom K electrons, with $Z_{2K} = Z_2 - 0.3$ and v_0 the Bohr velocity, one expects Coulomb ionization to occur most probably at p values of order $q_0^{-1} = v_1/\omega_{2K}$, where $\hbar\omega_{2K}$ is the K -shell ionization energy. That is, low-ve-

locity Coulomb excitation proceeds in a domain that is small compared to the K -shell radius $a_{2K} = Z_{2K}^{-1}a_0$ (a_0 being the Bohr radius).³ It follows that projectiles such that $Z_1/Z_2 \ll 1$ can only cause Coulomb excitation of K shells even at the lowest velocities because the projectile K electrons with shell radii $a_{1K} = Z_{1K}^{-1}a_0 \gg a_{2K}$, which could have caused Pauli excitation, remain outside the interaction region. By contrast, Pauli excitation presumably can occur when $Z_1 \approx Z_2$ as long as the wave functions of the target and the projectile electrons overlap, i.e., over ranges $p \lesssim a_{1K} + a_{2K}$, if judged by the size of the measured cross sections.⁴ Evidence for such large ranges of effective impact parameters has been found for L -shell x rays, under conditions where Pauli excitation of L shells via level crossings can be expected.⁹

A proton beam from a Van de Graaff accelerator was collimated to $\pm 0.07^\circ$ with two circular collimators of 0.254 mm diam, placed 20 cm apart. The final collimator was followed after 6 cm by a scraper slit of diameter 0.381 mm. The beam then passed through the target and an annular detector and stopped 50 cm from the target in a Faraday cup.

Protons scattered at an angle of 5.1° were detected by a 300- μm -thick Si annular detector at 5 cm from the target, with an angular acceptance of 1.0° . Background in the absence of a target was negligible compared to the counting rate with the target in place. X rays were detected at 90° to the beam direction with NaI(Tl) scintillation detectors coupled to RCA 8875 and 8850 photomultipliers. A 6-mm crystal with a 0.125-mm Be entrance window was used for the Ni and Ag targets, and a 0.025-mm window for the Al and Ca targets. A 0.5-cm² Si detector at 135° to the incident beam monitored the beam current through back-scattered protons. The targets of Al, Ca, Ni, and Ag, of thickness $\sim 100 \mu\text{g}/\text{cm}^2$ and tilted 45° relative to the beam and the x-ray detector, were either self-supporting (Ag, Ni), or were evaporated on 20- $\mu\text{g}/\text{cm}^2$ carbon foils. The targets were kept thin so as to minimize multiple-scattering effects and corrections for proton-energy losses.

Measurements were made for proton energies ranging from 0.3 to 3.0 MeV of the number of coincidences between the protons scattered at 5.1° and the K x rays produced in the scattering. The standard electronics for the coincidence measurements had resolving times from 2 to 40 nsec depending on the x-ray energy. The number

of scattered protons was determined from the annular-counter pulse-height spectrum. The monitor-counter data served as a check and determined the relative contribution of the carbon backing for the Al and Ca targets.

The main experimental difficulties arose from the large differences in the counting rates in the two detectors caused by the large differences between the Rutherford-scattering cross section and the x-ray production cross section. Beam currents, if kept to 10^{-11} – 10^{-13} A, yielded good true-to-accidental coincidence ratios, but this required very long running times, of the order of 2 days per point at low proton energies.

At each proton energy E_1 , or proton velocity v_1 , where $E_1(\text{keV}) = 25v_1^2(\text{a.u.})$, the absolute differential K -shell ionization cross section $d\sigma_K/d\Omega$, for a proton scattered at a laboratory angle of 5.1° , is obtained from the data N_c and N_s in the form

$$\frac{(d\sigma_K/d\Omega)_{5^\circ}}{(d\sigma_R/d\Omega)_{5^\circ}} = \gamma_K \frac{N_c}{N_s} \frac{4\pi}{\Omega_X \epsilon_X}, \quad (1)$$

where N_c and N_s are the number of coincidence counts and of single proton counts, respectively; γ_K is the fluorescence yield, $d\sigma_R/d\Omega$ the Rutherford scattering cross section, and Ω_X the solid angle subtended by the x-ray detector with efficiency ϵ_X . The absolute cross sections are estimated to have uncertainties of about ± 20 – 30% for the Ni, Ag, and Ca data and about $\pm 50\%$ for the Al point. The relative values for each element determined from the statistical uncertainties were generally better than $\pm 5\%$, but in a few instances were as large as $\pm 20\%$.

We compare the experiments with the semiclassical theory of Bang and Hansteen.³ We introduce the variable $x \equiv pq_0 \equiv (p/a_{2K})\xi_K^{-1}$, where $\xi_K \equiv (v_1/\omega_{2K})a_{2K}^{-1} \equiv v_1/\frac{1}{2}\theta_K v_{2K}$ is the universal projectile-velocity variable for K -shell ionization,¹ with $\theta_K = \hbar\omega_{2K}/Z_{2K}^2R$ ($R = 1 \text{ Ry} = 13.6 \text{ eV} = \frac{1}{2} \text{ a.u.}$). After integration over final states,¹⁰ the differential cross section for K -shell ionization by particles passing the target nucleus in the interval between x and $x + dx$ is given by

$$d\sigma_K(x, \xi_K) = (\sigma_{0K}/\theta_K)F(\xi_K)2\pi x P(x) dx \quad (2)$$

in terms of $\sigma_{0K} \equiv 8\pi a_{2K}^2 (Z_1/Z_{2K})^2$. The function $F(\xi_K)$ is tabulated.⁸ For $\xi_K \ll 1$, in the semiclassical and the plane-wave Born approximations^{3,11}

$$F(\xi_K) \frac{1}{\xi_K} \xrightarrow{\xi_K \ll 1} F_0(\xi_K) = (2^9/45)\xi_K^3. \quad (3)$$

In the following we use the reduced form $f(\xi_K) \equiv F(\xi_K)/F_0(\xi_K)$; approximately for $\xi_K \lesssim 1$, with er-

rors $< 1\%$, $f(\xi_K) = (1 + 1.72\xi_K^2)^{-4}$. The ionization probability

$$P(x) = \frac{45x^7}{2^6\pi} \int_x^\infty \frac{K_2^2(x') dx'}{x'^4}, \quad (4)$$

normalized as $2\pi \int_0^\infty xP(x) dx = 1$, can be computed with errors $< 1\%$ from the formula

$$P(x) = (45/2^6\pi)^{1/7} (1 + 1.96x + \frac{7}{16}\pi x^2) \exp(-2x). \quad (5)$$

Although (4) is strictly valid only when $\xi_K \ll 1$, it serves as a guide for $\xi_K \approx 1$. The variable p depends on ϑ as $p = d \cot(\vartheta/2)$, where $d \approx M_1 Z_1 Z_{2K} e^2 / 2ME_1$ with $M = (M_1^{-1} + M_2^{-1})^{-1}$. The experiment, by (1), yields

$$\left(\frac{d\sigma_K/d\Omega}{d\sigma_R/d\Omega} \right)_\vartheta = \frac{d\sigma_K/dp}{2\pi p} = \sigma_K(\xi_K) P(x) q_0^2 = \frac{2^{16} \pi f(\xi_K) Z_1^4}{45 \theta_K^5 Z_{2K}^2} \left(\frac{m_e}{M} \right)^2 \cot^2\left(\frac{\vartheta}{2}\right) \frac{P(x)}{x^2}. \quad (6)$$

It should depend on the impact parameter in a comprehensive way as given by the expression $x^{-2}P(x)$.

We introduce two improvements in Eq. (6).^{1,12} To account for the Coulomb deflection of the projectile in an approximate manner, we replace p in $P(x)$ by a mean distance of closest approach $p' = cp$ and thus x by cx , where $c = [(\gamma d/p)^2 + 1]^{1/2} + \gamma d/p$; the factor γ accounts for the difference between the straight line and hyperbolic trajectory in an average manner.¹³ For our condition, $\vartheta = 5.1^\circ$, $c = 1.046$ in the "straight-line" approximation where $\gamma = 1$; we set $c = 1.15$, as adjusted to the hyperbolic Coulomb deflection where $\gamma \sim \pi$.¹³ One incorporates the binding of the K -shell electrons to the projectile¹² by replacing θ_K with $\epsilon(p'/a_{2K})\theta_K$ and thus cx with $c\epsilon x$ where the function ϵ is given by, approximately,

$$\epsilon(z) = 1 + (2Z_1/\theta_K Z_{2K} z) [1 - (1+z) \exp(-2z)].$$

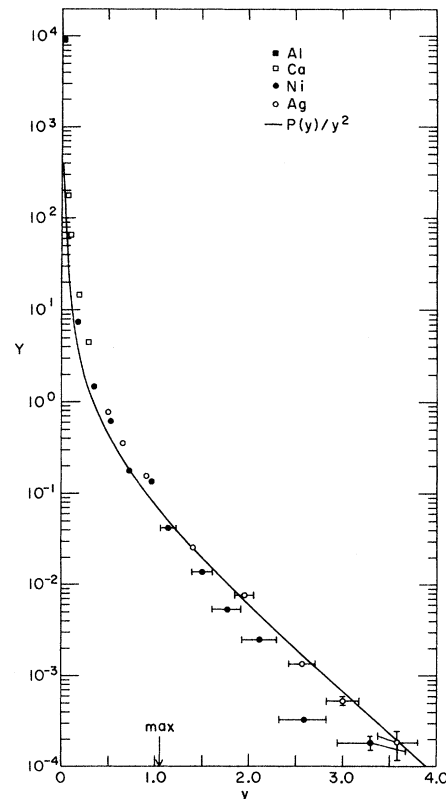
It is instructive, then, to plot the measured left-hand side of (6) in the form

$$Y = \left[\frac{2^{16} \pi c^2 f(\xi_K/\epsilon)}{45 (\epsilon \theta_K)^5} \frac{Z_1^4}{Z_{2K}^2} \left(\frac{m_e}{M} \right)^2 \cot^2\left(\frac{\vartheta}{2}\right) \right]^{-1} \left(\frac{d\sigma_K/d\Omega}{d\sigma_R/d\Omega} \right)_\vartheta \quad (7)$$

versus $y \equiv c\epsilon x$ and compare with $y^{-2}P(y)$. The result is shown in Fig. 1. The data Y for all targets, ranging over nearly 8 orders of magnitude, form a common experimental curve with a scatter comparable to their experimental uncertainties. We find that the data reported² on Cu, Se, and Ag from the angular distribution of scattered protons at fixed energies follow our data closely if scaled according to Eq. (7). The locus of the points coincides with the theoretical curve for $y \gtrsim 0.5$. At small y values the Y data rise above the curve. Here $\xi_K \rightarrow 1$, and the asymptotic form (4) should only be viewed as a tentative theoretical guide. The semiclassical approach is valid in the sense that the de Broglie wavelength of the particle, $\lambda_1 = \hbar/M_1 v_1$, is always small compared to $p = d \cot(\vartheta/2)$.

In summary, the semiclassical impact-param-

FIG. 1. Experimental data reduced as prescribed by Eq. (7), Y versus $y \equiv c\epsilon x$. The curve represents $y^{-2}P(y)$, based on Eq. (4). The arrow points to the value $y = 1.05$, where the distribution $2\pi y P(y)$ has its maximum. Fluorescence yields of 0.038, 0.163, 0.414, and 0.834 were used for Al, Ca, Ni, and Ag, respectively [W. Bambynek *et al.*, Rev. Mod. Phys. 44, 716 (1972)].



eter-dependent cross section for Coulomb K -shell ionization by slow particles is confirmed in detail with protons by coincidence measurements between the emerging scattered particles and the characteristic target K -shell x rays emitted in the process of filling the K -shell hole created by the penetrating particle. This provides a well-documented basis for the quantitative search of impact-parameter-dependent deviations that must occur when $Z_1 \rightarrow Z_2$ and Pauli excitation of the K shell becomes dominant.

One of us (W.B.) had the benefit of discussions with G. Basbas, L. C. Feldman, and R. Laubert.

*Work performed under the auspices of the U. S. Atomic Energy Commission.

†Permanent address: Department of Physics, New York University, New York, N. Y. 10003.

¹W. Brandt, in *Proceedings of the International Conference on Inner-Shell Ionization Phenomena, Atlanta, Georgia, April 1972*, edited by R. W. Fink, S. T. Manson, M. Palms, and P. V. Rao (U. S. Atomic Energy Commission, Oak Ridge, Tenn., 1973), p. 948.

²E. Laegsgaard, J. V. Andersen, and L. C. Feldman, in *Proceedings of the International Conference on Inner-Shell Ionization Phenomena, Atlanta, Georgia, 1972*, edited by R. W. Fink *et al.* (U. S. Atomic Energy Commission, Oak Ridge, Tenn., 1973), and Phys. Rev. Lett.

29, 1206 (1972).

³J. Gang and J. M. Hansteen, Kgl. Dan. Vidensk. Selsk., Mat.-Fys. Medd. 31, No. 13 (1959).

⁴W. Brandt and R. Laubert, Phys. Rev. Lett. 24, 1037 (1970).

⁵W. Brandt, in *Proceedings of the Third International Conference on Atomic Physics, Boulder Colorado, August 1972*, edited by S. J. Smith (Plenum, New York, to be published).

⁶M. Barat and W. Lichten, Phys. Rev. A 6, 211 (1972).

⁷F. P. Larkins, J. Phys. B: Proc. Phys. Soc., London 5, 571 (1972).

⁸G. Basbas, W. Brandt, and R. Laubert, Phys. Rev. A (to be published).

⁹H. J. Stein, H. O. Lutz, P. H. Mokler, K. Sistemich, and P. Armbruster, Phys. Rev. Lett. 24, 701 (1970), and Phys. Rev. A 2, 2575 (1970), and 5, 2126 (1972).

¹⁰Integration of Eq. (3.12), Ref. 3, over final states E_f .

¹¹T. Huus, J. H. Bjerregaard, and B. Elbek, Kgl. Dan. Vidensk. Selsk., Mat.-Fys. Medd. 30, No. 13 (1956).

¹²W. Brandt, R. Laubert, and I. Sellin, Phys. Lett. 21, 518 (1966), and Phys. Rev. 151, 56 (1966).

¹³Note that integration of Eq. (2) with $P(cx)$ yields a correction factor for Coulomb deflection, $G(q_0 d) = 2\pi \times \int_0^\infty P(cx)x dx = 2\pi \int_{2q_0 d}^\infty P(x')(x' - q_0 d) dx'$, to the cross section $\sigma_K(\xi_K)$, Eq. (3). It represents a "straight-line" approximation, and becomes essentially equal to the factor $9E_{10}(\pi q_0 d)$ for a hyperbolic trajectory as derived earlier (Ref. 12) if one sets $G(q_0 \gamma d)$ with $\gamma \sim \pi$ in our range of x values.

Photomagnetic Positronium-Spin Conversion in Solids*

Werner Brandt and Paul Kliauga

Department of Physics, New York University, New York, New York 10003

(Received 12 December 1972)

We have observed spin conversion of orthopositronium and parapositronium in interaction with photoexcited, metastable, paramagnetic triplet states of phosphorescent molecules in rigid solutions, through changes in the positron lifetime spectra induced by light. The results bear on the statistics of the spin conversion processes, and on the diffusion of positronium in solids.

Phosphorescence of organic molecules in solid solutions is attributed to the slow (relative to fluorescence) emission of light in symmetry-forbidden transitions from the lowest paramagnetic triplet state T (spin quantum number $S = 1$) to the diamagnetic singlet ground state ($S = 0$).^{1,2} Photomagnetism was first demonstrated in the pioneering work of Lewis, Calvin, and Kasha³ through measurements of the magnetic susceptibility of phosphorescent solids under illumination. Since then, the properties of molecular triplet states have been investigated extensively by electron-spin resonance and in the framework of exciton physics.⁴

We report first observations of the photomagnetic spin conversion of orthopositronium o -Ps (electron and positron spins parallel, $S = 1$) and of parapositronium p -Ps (electron and positron spins antiparallel, $S = 0$) in interaction with molecules in photoexcited triplet states, imbedded in rigid diamagnetic matrices. Our results open the possibility for measurements of the spin-statistic probabilities of ortho-to-para and of para-to-ortho positronium conversion. Moreover because of its monotonic dependence on the light intensity, spin conversion provides a flexible new method for the study of Ps propagation in solids through the interaction with conversion